A MISMATCHED BOUND FOR STOCHASTIC DOA ESTIMATION

Gerald LaMountain and Pau Closas

Dept. of Electrical & Computer Engineering, Northeastern University, Boston, MA (USA)
e-mail: {lamountain.g, closas}@northeastern.edu

2020 54th Asilomar Conference on Signals, Systems, and Computers | 978-0-7381-3126-9/20/$31.00 ©2020 IEEE | DOI: 10.1109/IEEECONF51394.2020.9443348

ABSTRACT

Model misspecification occurs when the assumed model on which an estimator is derived differs from the true underlying model for a given set of data. This often occurs when, for reasons of practicality, it is not reasonable to account for all of the real-world factors affecting a given signal. In the context of radio direction-of-arrival (DOA) estimation this can occur due to interference, multipath or other unanticipated phenomena, or due to modelling assumptions that are made in order to utilize computationally efficient array processing algorithms. In this contribution we address the problem of model misspecification in the context of multi-antenna stochastic direction-of-arrival estimation. We present this problem as an application for the Misspecified Cramér-Rao lower bound (MCRB) and derive a set of general models and expressions for computing the MCRB for the misspecified stochastic DOA problem. These models are compared against the convergent results of the stochastic maximum-likelihood (ML) estimation to show that the performance of an asymptotically optimal unbiased estimator does converge to the value predicted by the MCRB.

Index Terms— Model misspecification, Cramér-Rao lower bound, multi sensor array processing, direction-of-arrival estimation, stochastic maximum-likelihood.

1. MOTIVATION & SIGNAL MODELS

The objective of this paper is in providing a framework for addressing the impact of model misspecification on the problem of direction-of-arrival (DOA) estimation using multi-sensor antenna arrays [1]. Radio direction finding is a classic problem in multi-sensor array processing with research dating back nearly a hundred years. Over this time various high-resolution techniques have been developed based on a number of different estimation approaches: from various flavors of maximum likelihood to computationally efficient eigenspace methods. Among these, maximum likelihood techniques represent a sort of "gold standard" for unbiased estimators, as they have been shown to asymptotically attend the theoretical minimum estimation error provided by the Cramér-Rao lower bound [2]. These techniques require a complete characterization of the model from which the observed data is generated. In many practical applications however, this is either infeasible due to environmental variability or impractical due to computational limitations that arise from model complexity. In both cases it may be possible to circumvent these issues by applying a simplified model which violates the "complete characterization" requirement. This will inevitably result in a loss of estimation precision and accuracy based on the level of simplification and the degree of mismatch between the assumed model and the statistical characteristics of the observed data. It is important then to be able to identify a lower bound on the performance of an estimator based on this "mismatched model," so that practical design considerations can be made in selecting the right estimator for a given application. With respect to the radio direction-of-arrival problem, we propose using the "stochastic maximum likelihood" estimator and associated stochastic model as the base class of assumed model estimator, and identify a set of equations based on the Misspecified Cramér-Rao lower bound (MCRB) [3–7] which can be used to quantify the performance of this misspecified estimator when applied to data from various DOA applications [8–11].

1.1. Assumed and Generalized DOA models

The stochastic maximum-likelihood (SML) model is proposed as the baseline "assumed model" for multiple reasons. First, in contrast to the deterministic maximum-likelihood (DML) model, the explicit structure of the observed signal is not required, only the statistical characterization of the observations. In this way, the statistical model can be applied to adversarial scenarios where the structure of the incoming signals is variable or can not be known. Second is that estimators based on the DML model have been shown *not* to attend the Cramér-Rao lower bound as the number of observations goes to infinity. This is because the number of unknowns scales with the number of observations leading to a situation where the Cramér-Rao lower bound can no longer be used to predict estimator performance.

Consider a single stochastic narrowband signal source located at angle $\boldsymbol{\theta}$ with respect to the reference position of an array of M sensors. The observation vector for the k^{th} snap-

This work has been partially supported by the National Science Foundation under Awards CNS-1815349 and ECCS-1845833.

shot is modelled as

$$\mathcal{M}_1 : \mathbf{x}_k = \mathbf{d}(\boldsymbol{\theta})a_k + \mathbf{n}_k,\ k = 1, 2, \ldots, K \tag{1}$$

The scalar signal amplitude a_k is assumed to be zero-mean circularly stationary complex Gaussian random value with covariance σ_s^2, such that $a \sim \mathcal{CN}(0, \sigma_s^2)$. The additive noise random value n_k is also assumed to be a zero-mean circularly stationary complex Gaussian random variable with covariance given by $\sigma_n^2 \boldsymbol{I}$. The signal values are modified by the array steering vector $\mathbf{d}(\boldsymbol{\theta})$ such that the observation vector $\mathbf{x}_k$ also comes from a circularly symmetric complex normal distribution $\mathbf{x}_k \sim \mathcal{CN}(\boldsymbol{\mu}_{x_1}, \boldsymbol{\Sigma}_{x_1})$ [12]. The moments of this distribution are then related to the parameter vector $\boldsymbol{\theta}$ by way of the steering vector such that

$$\boldsymbol{\mu}_{x_1} = \mathbb{E}\{\mathbf{x}_k\} = \mathbf{0} \tag{2}$$

$$\boldsymbol{\Sigma}_{x_1} = \mathbb{E}\{\mathbf{x}_k \mathbf{x}_k^H\} = \sigma_s^2 \mathbf{d}(\boldsymbol{\theta})\mathbf{d}(\boldsymbol{\theta})^H + \sigma_n^2 \boldsymbol{I} \tag{3}$$

This assumed model is an incomplete, or incorrect characterization of the true distribution of the observations $\mathbf{x}_k$. In general, it is not possible or necessary to explicitly identify the entirety of the "true" model, however we will make some assumptions about its structure which are broadly applicable to the problem of DOA estimation. For the sake of comparison, we consider a true model of the form

$$\mathcal{M}_0 : \mathbf{x}_k = \mathbf{D}(\boldsymbol{\theta})\mathbf{a}_k + \mathbf{n}_k \tag{4}$$

This model differs from the assumed model in that, rather than a single realization of scalar a, the array observes a vector of dependent realizations $\mathbf{a}$ related by the matrix of *known* correlations $\mathbf{R}_s$ such that $\mathbf{a} \sim \mathcal{CN}(\mathbf{0}, \sigma_s^2 \mathbf{R}_s)$. This results in observations in the same space as the assumed model $\mathcal{M}_1$, but distributed according to a complex normal distribution with moments

$$\boldsymbol{\mu}_{x_0} = \mathbb{E}\{\mathbf{x}_k\} = \mathbf{0} \tag{5}$$

$$\boldsymbol{\Sigma}_{x_0} = \mathbb{E}\{\mathbf{x}_k \mathbf{x}_k^H\} = \sigma_s^2 \mathbf{d}(\boldsymbol{\theta})\mathbf{R}_s \mathbf{d}(\boldsymbol{\theta})^H + \sigma_n^2 \boldsymbol{I} \tag{6}$$

It's important to note that in the case of this "true" model the correlations given by $\mathbf{R}_s$ are considered "known," while in practical applications these correlations would likely be unknown and need to be estimated, adding additional complexity to the parameter estimation problem. For the purposes of analyzing the mismatch between the true data distribution and the simplified assumed distributions given by $\mathcal{M}_1$ however, we can test the mismatch for multiple different values of $\mathbf{R}_s$ in order to understand the relationship between estimation error and correlation. Note that there exists an important limit case where the two models are statistically identical, which occurs when $\mathbf{R}_s$ is the all ones matrix. Under this condition the two models are said to be "matched" and the performance of estimators based on the assumed model can be completely characterized by standard analysis of the properties of that model alone, for example using the standard Cramér-Rao lower bound.

1.2. Use Case: Deterministic Plane-Wave Signal

In order to understand how these models might appear in a practical scenario, we wish to analyze the case where the observed signal is not random, but instead a continuous plane wave. In this case, we can compute the correlations $\mathbf{R}_s$ between the signals observed at each of the array elements as a function of the antenna spacing and the frequency of the impinging wave. The ith antenna located at position $\boldsymbol{p}_i$ observes the signal $s(t+\tau_i(t))$, where $\tau_i(t)$ is the propagation delay of the ith sensor with respect to the the reference position of the antenna, computed as

$$\tau_i = \frac{\rho_i(t)}{c} = \frac{\hat{\mathbf{r}}_\psi^\top \mathbf{p}_i(t)}{c} \tag{7}$$

where $\rho_i(t)$ is the additional propagation path produced by projecting the antenna position onto the unit vector $\hat{\mathbf{r}}_\psi$ pointing towards the signal source. From this, we then compute the correlation of the signals observed at antennas i and j respectively as

$$\tau_{i,j} = \frac{\Delta\rho_{i,j}(t)}{c} = \frac{\hat{\mathbf{r}}_\psi^\top (\mathbf{p}_i(t) - \mathbf{p}_j(t))}{c} \tag{8}$$

For a given signal waveform $s(t)$, the correlation between antenna elements can be computed as

$$[\mathbf{C}_s]_{i,j} = \int_{-\infty}^{\infty} s(t - \tau_{i,j}(t))\bar{s}(t) \tag{9}$$

and finally, the covariance for the true model given in (4) can be computed from these correlations. By way of an example, we consider an incoming signal of the form

$$a(t) = A \sin(2\pi f_c t) \tag{10}$$

The correlation of the measurements at each sensor is then given by

$$[\mathbf{C}_s]_{i,j} = \cos(2\pi f_c \tau_{i,j}) \tag{11}$$

and for sufficiently high sample rates $f_s >> f_c$ and sample size K, the observations at the array can be accurately modelled using (4) with $\sigma_s^2 = A^2$ and $\mathbf{R}_s = \mathbf{C}_s/2$. In the following sections we will discuss the characteristics of applying an estimator derived from $\mathcal{M}_1$ as described in (1) instead of the more descriptive model $\mathcal{M}_0$.

2. ESTIMATOR PERFORMANCE UNDER THE PROPOSED DATA MODELS

2.1. Mean Characteristics Stochastic DOA Estimation

We consider estimators for the assumed model which are misspecified unbiased (MS-unbiased). As described in the literature, this property states that the estimator must be unbiased with respect to the “pseudotrue parameter” for the assumed and true models. The pseudotrue parameter is in turn defined as the *unique* interior point $\tilde{\boldsymbol{\xi}}_0 \in \boldsymbol{\Xi}$ that minimizes the KL divergence between output distributions for the true and assumed models with respect to the data $\mathbf{x}$ and the true parameter $\boldsymbol{\xi}_0$

$$\tilde{\boldsymbol{\xi}}_0 = \arg\min_{\boldsymbol{\xi}} \ \mathcal{D}(p(\mathbf{x})||f(\mathbf{x}|\boldsymbol{\xi})) \tag{12}$$

In the case of the stochastic models $\mathcal{M}_1$ and $\mathcal{M}_0$, and with unknowns $\boldsymbol{\xi} = [\boldsymbol{\theta}, \sigma_s^2]^\top$, these distributions are

$$p(\mathbf{x}) = \mathcal{CN}(\mathbf{0}, \boldsymbol{\Sigma}_{x_0})\big|_{\boldsymbol{\xi}=\boldsymbol{\xi}_0} \tag{13}$$

$$f(\mathbf{x}|\boldsymbol{\xi}) = \mathcal{CN}(\mathbf{0}, \boldsymbol{\Sigma}_{x_1}) \tag{14}$$

The pseudotrue parameter is not in general consistent with the true parameter $\boldsymbol{\xi}$, however it does represent the optimum to which we can expect our unbiased estimator to converge. It holds then that

$$\mathbb{E}_p\{\hat{\boldsymbol{\xi}}(\mathbf{x})\} = \int \hat{\boldsymbol{\xi}}(\mathbf{x})p(\mathbf{x})d\mathbf{x} = \boldsymbol{\xi}_0 \tag{15}$$

which provides us with a means of evaluating the MS-unbiasedness of a given estimator. That the stochastic maximum likelihood estimator described in the DOA literature adheres to the MS-unbiasedness property described in (15) is a classical result which follows from a series of assumptions closely related to the MLE consistency result of LeCam [13]. Computation of the pseudotrue parameter for our models, then is a matter of numerically solving (17) for its unique solution. Expanding (17) using the expression for complex valued zero-mean Gaussian distributions, we find that the pseudotrue parameter is given by

$$\tilde{\boldsymbol{\xi}} = \arg\min_{\boldsymbol{\xi}} \left\{ \log \frac{|\boldsymbol{\Sigma}_{x_1}|}{|\boldsymbol{\Sigma}_0|} + \mathrm{Tr}\left\{\boldsymbol{\Sigma}_{x_1}^{-1}\boldsymbol{\Sigma}_0\right\} \right\} \tag{16}$$

$$= \arg\min_{\boldsymbol{\xi}} \left\{ \log|\boldsymbol{\Sigma}_{x_1}| + \mathrm{Tr}\left\{\boldsymbol{\Sigma}_{x_1}^{-1}\boldsymbol{\Sigma}_0\right\} \right\} \tag{17}$$

where $\boldsymbol{\Sigma}_0 = \boldsymbol{\Sigma}_{x_0}|_{\boldsymbol{\xi}=\boldsymbol{\xi}_0}$ is the true covariance of the observations, no longer parameterized by $\boldsymbol{\xi}$. For the model given in (1), the canonical SML solution is given by maximization of the likelihood function [12]

$$\hat{\boldsymbol{\xi}} = \arg\max_{\boldsymbol{\xi}} \left\{ -\log|\boldsymbol{\Sigma}_{x_1}| - \sum_{k=1}^{K} \mathbf{x}_k^H \boldsymbol{\Sigma}_{x_1}^{-1} \mathbf{x}_k \right\} \tag{18}$$

$$= \arg\min_{\boldsymbol{\xi}} \left\{ \log|\boldsymbol{\Sigma}_{x_1}| + \mathrm{Tr}\{\boldsymbol{\Sigma}_{x_1}^{-1}\mathbf{S}\} \right\} \tag{19}$$

where $\mathbf{S}$ is the sample covariance given by

$$\mathbf{S} = \frac{1}{K}\sum_{k=1}^{K} \mathbf{x}_k^H \mathbf{x}_k \tag{20}$$

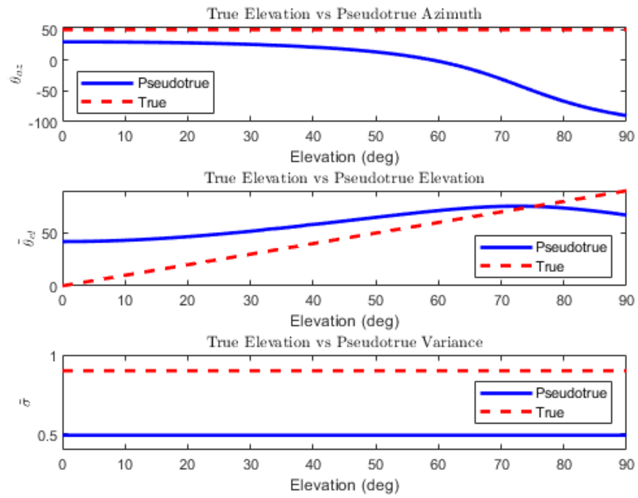

Fig. 1. Pseudotrue parameter vs True parameters for various True elevation values.

Figure 1 shows an example of how the pseudotrue parameter changes with respect to the true parameter. Azimuth, signal variance and signal correlation were held constant while the true elevation was varied. The correlations were assigned such that each sensor was strongly correlated or anti-correlated with each of the seven the other sensors based on the distance between them. The pseudotrue values for each of the parameters is clearly not consistent with the true DOA over much of the region, however the underspecified model still provides a useful estimate at certain elevations.

2.2. Performance of MS Stochastic DOA Estimation

In order to fully characterize the performance of the DOA stochastic ML estimator under model misspecification, we need to be able to evaluate the optimal variance of the computed estimates as well as the mean. This is where estimation bounds come in, and in particular the Misspecified Cramér-Rao lower bound (MCRB). The MCRB is a generalization of the classical Cramér-Rao lower bound, which has become widespread as a means of evaluating the performance of estimators by providing the “best case” estimator variance. In particular, it can be shown that an optimal unbiased estimator will asymptotically adhere to the CRB as the number of data points or signal-to-noise ratio go to infinity. In a similar way, it can be expected that an optimal MS-unbiased estimator will be bounded in performance by the MCRB.

The MCRB is computed from a generalization of the Fisher Information Matrix (FIM) given by matrices $[\boldsymbol{A}_{\tilde{\boldsymbol{\xi}}}]$ and

$[\boldsymbol{B}_{\tilde{\xi}}]$ constructed from the model derivatives as

$$[\boldsymbol{A}_{\tilde{\xi}}]_{ij} \equiv [\mathbb{E}_p\{\nabla_\xi \nabla_\xi^\top \ln f(\boldsymbol{x}|\boldsymbol{\xi})\}]_{ij} \tag{21}$$

$$= \mathbb{E}_p\left\{ \frac{\partial^2}{\partial \xi_i \partial \xi_j} \ln f(\boldsymbol{x}|\boldsymbol{\xi}) \bigg|_{\boldsymbol{\xi}=\tilde{\boldsymbol{\xi}}} \right\} \tag{22}$$

$$[\boldsymbol{B}_{\tilde{\xi}}]_{ij} \equiv [\mathbb{E}_p\{\nabla_\xi \ln f(\boldsymbol{x}|\boldsymbol{\xi}) \cdot \nabla_\xi^\top \ln f(\boldsymbol{x}|\boldsymbol{\xi})\}]_{ij} \tag{23}$$

$$= \mathbb{E}_p\left\{ \frac{\partial \ln f(\boldsymbol{x}|\boldsymbol{\xi})}{\partial \xi_i}\bigg|_{\boldsymbol{\xi}=\tilde{\boldsymbol{\xi}}} \cdot \frac{\partial \ln f(\boldsymbol{x}|\boldsymbol{\xi})}{\partial \xi_j}\bigg|_{\boldsymbol{\xi}=\tilde{\boldsymbol{\xi}}} \right\} \tag{24}$$

The required model derivatives are computed from the expanded forms of the Gaussian distributions in (13,14) [14]. The resulting expression for $[\boldsymbol{A}_{\tilde{\xi}}]$ is given by

$$\begin{aligned} \mathbb{E}_p\left\{ \frac{\partial^2 \ln f(\boldsymbol{x}|\boldsymbol{\xi})}{\partial \xi_i \partial \xi_j} \right\} &= \\ \mathrm{Tr}\left\{ -\boldsymbol{\Sigma}_{x_1}^{-1} \frac{\partial^2 \boldsymbol{\Sigma}_{x_1}}{\partial \xi_i \partial \xi_j} (\boldsymbol{I} - \boldsymbol{\Sigma}_{x_1}^{-1}\boldsymbol{\Sigma}_0) \right\} & \\ + \mathrm{Tr}\left\{ + \boldsymbol{\Sigma}_{x_1}^{-1} \frac{\partial \boldsymbol{\Sigma}_{x_1}}{\partial \xi_i} \boldsymbol{\Sigma}_{x_1}^{-1} \frac{\partial \boldsymbol{\Sigma}_{x_1}}{\partial \xi_j} \boldsymbol{\Sigma}_{x_1}^{-1}\boldsymbol{\Sigma}_0 \right\} & \\ + \mathrm{Tr}\left\{ \boldsymbol{\Sigma}_{x_1}^{-1} \frac{\partial \boldsymbol{\Sigma}_{x_1}}{\partial \xi_j} \boldsymbol{\Sigma}_{x_1}^{-1} \frac{\partial \boldsymbol{\Sigma}_{x_1}}{\partial \xi_i} (\boldsymbol{I} - \boldsymbol{\Sigma}_{x_1}^{-1}\boldsymbol{\Sigma}_0) \right\} & \end{aligned} \tag{25}$$

while the expression for $[\boldsymbol{B}_{\tilde{\xi}}]$ is given by

$$\begin{aligned} \mathbb{E}_p\left\{ \frac{\partial \ln f(\boldsymbol{x}|\boldsymbol{\xi})}{\partial \xi_i} \cdot \frac{\partial \ln f(\boldsymbol{x}|\boldsymbol{\xi})}{\partial \xi_j} \right\} &= \\ \mathrm{Tr}\left\{ \boldsymbol{\Sigma}_{x_1}^{-1} \frac{\partial \boldsymbol{\Sigma}_{x_1}}{\partial \xi_i} \right\} \mathrm{Tr}\left\{ \boldsymbol{\Sigma}_{x_1}^{-1} \frac{\partial \boldsymbol{\Sigma}_{x_1}}{\partial \xi_j} \right\} & \\ + \mathrm{Tr}\left\{ \boldsymbol{\Sigma}_{x_1}^{-1} \frac{\partial \boldsymbol{\Sigma}_{x_1}}{\partial \xi_i} \right\} \mathrm{Tr}\left\{ \boldsymbol{Q}_j \boldsymbol{\Sigma}_0 \right\} & \\ + \mathrm{Tr}\left\{ \boldsymbol{\Sigma}_{x_1}^{-1} \frac{\partial \boldsymbol{\Sigma}_{x_1}}{\partial \xi_j} \right\} \mathrm{Tr}\left\{ \boldsymbol{Q}_i \boldsymbol{\Sigma}_0 \right\} & \\ - \mathrm{Tr}\left\{ \boldsymbol{Q}_i \boldsymbol{\Sigma}_0 \right\} \mathrm{Tr}\left\{ \boldsymbol{Q}_j \boldsymbol{\Sigma}_0 \right\} & \\ + \mathrm{Tr}\left\{ \boldsymbol{Q}_i \boldsymbol{\Sigma}_0 \boldsymbol{Q}_j \boldsymbol{\Sigma}_0 \right\} & \end{aligned} \tag{26}$$

with

$$\boldsymbol{Q}_i = \boldsymbol{\Sigma}_{x_1}^{-1} \frac{\partial \boldsymbol{\Sigma}_{x_1}}{\partial \xi_i} \boldsymbol{\Sigma}_{x_1}^{-1}, \quad \boldsymbol{Q}_j = \boldsymbol{\Sigma}_{x_1}^{-1} \frac{\partial \boldsymbol{\Sigma}_{x_1}}{\partial \xi_j} \boldsymbol{\Sigma}_{x_1}^{-1} \tag{27}$$

Finally, the error bound can be computed as

$$\mathrm{MSE}_p(\hat{\boldsymbol{\xi}}, \tilde{\boldsymbol{\xi}}) \equiv \mathbb{E}_p\{(\hat{\boldsymbol{\xi}} - \tilde{\boldsymbol{\xi}})(\hat{\boldsymbol{\xi}} - \tilde{\boldsymbol{\xi}})^\top\} \tag{28}$$

$$\geq \frac{1}{N}[\boldsymbol{A}_{\tilde{\xi}}^{-1} \boldsymbol{B}_{\tilde{\xi}} \boldsymbol{A}_{\tilde{\xi}}^{-1}] = \mathrm{MCRB}(\tilde{\boldsymbol{\xi}}) \tag{29}$$

Note that in the matched case this simplifies to the canonical FIM given by Slepian-Bangs formula

$$[\boldsymbol{J}_{\boldsymbol{\xi}}]_{ij} = N\,\mathrm{Tr}\left\{ \frac{\partial \boldsymbol{\Sigma}_{x_1}}{\partial \xi_i} \boldsymbol{\Sigma}_{x_1}^{-1} \frac{\partial \boldsymbol{\Sigma}_{x_1}}{\partial \xi_j} \boldsymbol{\Sigma}_{x_1} \right\} \tag{30}$$

3. RESULTS

In order to validate the pseudotrue parameter and performance bound derived in Section 2, performance of the SML estimator was evaluated using both data generated in simulation according to both the assumed and true models $\mathcal{M}_1$ and $\mathcal{M}_0$ as described in (1) and (4) respectively. For the true model, rather than observing a single realization of the pseudorandom signal a_k, each of the eight antenna elements in the simulated system observe independent realizations of the random parameter as a vector $\mathbf{a}_k$ multiplied by the diagonalization of the array steering vector $\mathbf{D} = \mathrm{diag}(\mathbf{d}(\boldsymbol{\theta}))$. Simulation was performed at various signal-to-noise ratios and different correlation values. In each case where the correlation was varied, the matrix $\mathbf{R}_s$ was specified by a Toeplitz matrix with one on the diagonal and uniform correlation r at each of the off-diagonal elements. The pseudotrue parameter and SML estimate were each computed according to (17) and (19) respectively using an unconstrained numerical optimization routine in MATLAB with a large number of evaluations, allowing for the highest level of convergence.

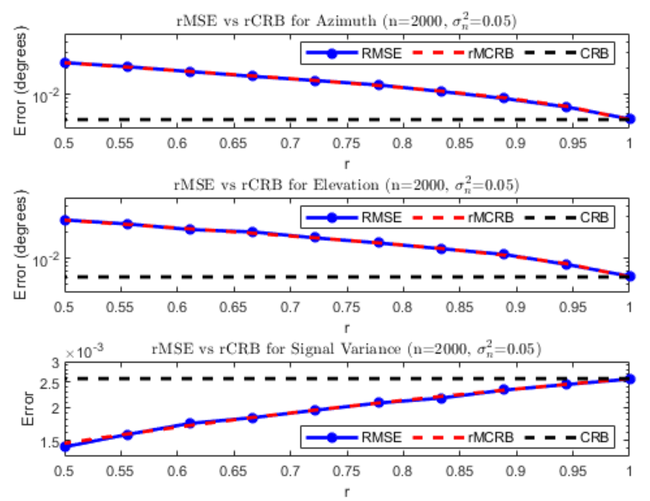

Fig. 2. Mismatched RMSE vs Correlation for (Top) Azimuth, (Middle) Elevation and (Bottom) signal variance. Also pictured, the "matched" Cramér-Rao lower bound showing the convergence of the MCRB to the CRB in the matched case where the observations are all perfectly correlated.

Figure 2 shows the results of varying the off-diagonal correlations, while Figure 3 shows the results of varying the signal-to-noise ratio. In each case, the MSE was computed as an average of $N = 2000$ Monte-Carlo iterations with respect to the computed psuedotrue parameter $\tilde{\boldsymbol{\xi}}$ to produce the "mismatched mean-squared error". This value was compared to the MCRB for each of the unknown parameters $\boldsymbol{\xi} = [\boldsymbol{\theta}, \sigma_s^2]^\top$ for azimuth, elevation and signal variance. In each case, it

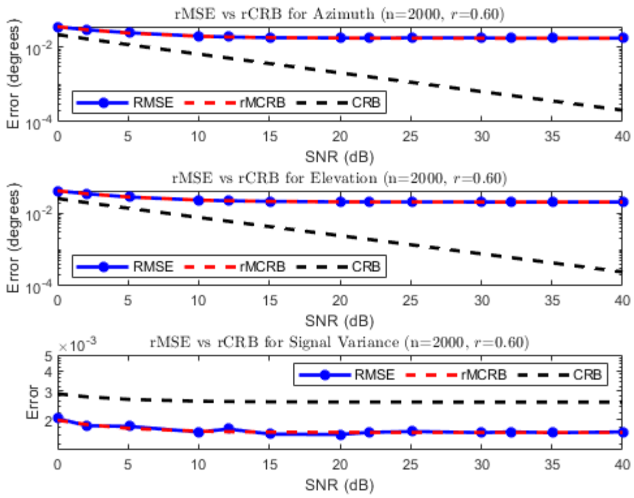

Fig. 3. Mismatched RMSE vs Signal-to-Noise ratio (dB) for (Top) Azimuth, (Middle) Elevation and (Bottom) signal variance. See (28).

was shown that the behavior of the estimator was to attend the MCRB even for relatively low SNR values, thus validating the expressions for the MCRB for the models described in this paper. Another thing to note from these figures is that the MCRB is *not* necessarily lower than the matched CRB in all cases. In Figure 2 the estimation error for the signal variance with respect to the *pseudotrue parameter* is lower than for the matched case. Even though this is the case, because of the bias introduced by the mismatch resulting in a larger gap between the pseudotrue and true parameters, the estimation error with respect to the *true parameter* would increase as correlation decreased. Both the estimation error with respect to the pseudotrue parameter (characterized by the MCRB) and the offset of the pseudotrue parameter with respect to the true parameter must be analyzed when determining whether or not the estimator meets the required performance specifications in the mismatched case.

4. CONCLUSIONS

In this contribution we've shown that the Misspecified Cramér-Rao Lower Bound can be used to bound the performance of MS-unbiased estimators where the distribution of the observations differs from that predicted by the assumed model. By evaluating the performance of a given estimator against a variety of such distributions, it is possible to determine the impact of certain kinds of model errors and evaluate the feasibility of the underlying assumptions behind them. We have discussed the application of this MCRB based approach to the problem of stochastic direction-of-arrival estimation. In 1.1 we proposed a fundamental "assumed model" based on the classical stochastic maximum likelihood (SML) approach, and a possible "true model" which expands upon the assumed to include asynchronous observations and other practical array phenomena. We have described the method by which the discrepancy between the two models might be evaluated using the MCRB. Additionally, in 1.2 we discussed how this methodology might be applied to the case where the observations are not stochastic, but instead follow a particular signal model. We described how this deterministic model can be considered as a limit case of the generalized stochastic model and subjected to the mismatch evaluation described in 2.1 and 2.2. Finally, we conclude that since the expressions in (25) and (26) apply generally to a certain class of Gaussian distributions, the methodology discussed can be broadly applied to different stochastic and deterministic data distributions.

5. REFERENCES

[1] Hamid Krim and Mats Viberg, "Two decades of array signal processing research: the parametric approach," *IEEE signal processing magazine*, vol. 13, no. 4, pp. 67–94, 1996.

[2] Petre Stoica and Arye Nehorai, "MUSIC, maximum likelihood, and Cramer-Rao bound," *IEEE Transactions on Acoustics, speech, and signal processing*, vol. 37, no. 5, pp. 720–741, 1989.

[3] Quang H Vuong, "Cramér-Rao bounds for misspecified models," 1986.

[4] Christ D Richmond and Larry L Horowitz, "Parameter bounds on estimation accuracy under model misspecification," *IEEE Transactions on Signal Processing*, vol. 63, no. 9, pp. 2263–2278, 2015.

[5] Stefano Fortunati, Fulvio Gini, and Maria S Greco, "The misspecified Cramér-Rao bound and its application to scatter matrix estimation in complex elliptically symmetric distributions," *IEEE Transactions on Signal Processing*, vol. 64, no. 9, pp. 2387–2399, 2016.

[6] Mahamadou Lamine Diong, Eric Chaumette, and François Vincent, "On the efficiency of maximum-likelihood estimators of misspecified models," in *2017 25th European Signal Processing Conference (EUSIPCO)*. IEEE, 2017, pp. 1455–1459.

[7] Stefano Fortunati, Fulvio Gini, Maria S Greco, and Christ D Richmond, "Performance bounds for parameter estimation under misspecified models: Fundamental findings and applications," *IEEE Signal Processing Magazine*, vol. 34, no. 6, pp. 142–157, 2017.

[8] C. Fernández-Prades, J. Arribas, and P. Closas, "Robust GNSS receivers by array signal processing: Theory and

implementation," *Proceedings of the IEEE*, vol. 104, no. 6, pp. 1207–1220, June 2016.

[9] Miguel Angel Ribot, Joaquin Cabeza, Pau Closas, Cyril Botteron, and Pierre-Andre Farine, "Estimation bounds for GNSS synthetic aperture techniques," in *2017 IEEE 7th International Workshop on Computational Advances in Multi-Sensor Adaptive Processing (CAMSAP)*. Dec. 2017, IEEE.

[10] Yu Hsuan Chen, Fabian Rothmaier, Dennis Akos, Sherman Lo, and Per Enge, "Towards a practical single element null steering antenna," Monterey, CA, 2017, Proc. of the Institute of Navigation International Technical Meeting.

[11] Gerald LaMountain and Pau Closas, "Maneuver Optimization for Synthetic Aperture based DOA estimation of GNSS Jammers," in *2020 IEEE/ION Position, Location and Navigation Symposium (PLANS)*. IEEE, 2020, pp. 44–49.

[12] A.G Jaffer, "Maximum likelihood direction finding of stochastic sources: a separable solution," in *ICASSP-88., International Conference on Acoustics, Speech, and Signal Processing*. 1988, pp. 2893–2896 vol.5, IEEE.

[13] Halbert White, "Maximum likelihood estimation of misspecified models," *Econometrica*, vol. 50, no. 1, pp. 1–25, 1982.

[14] Elie Bou Daher, "Analysis and design of nonuniform arrays for direction finding," 2018.